VIENNA 2016
30 May – 2 June 2016 | Reed Messe Wien

We SRS2 01

Subsea Karst Detection and Imaging Improvement Using Full Waveform Inversion

F. C. Loh* (CGG), B.L. Chuah (CGG), J. Zhou (CGG), T. Manning (BP), S. Wolfarth (BP) & D. Priyambodo (BP)

SUMMARY

This paper describes the construction of a high-resolution anisotropic FWI model that is used to help image a karstified carbonate layer (Faumai) and also to help define the underlying clastic reservoirs. The karst zones show extreme velocity rugosity. Conventional reflection tomography cannot resolve these anomalous velocities, and the seismic images below these karstified carbonates are distorted and are poor for interpretation.

In 2009 an isotropic FWI algorithm, up to 7Hz, was applied to this OBC survey by BP. Image quality was significantly improved. However, in and below the karst formation, the FWI velocity resolution improved less.

In 2015, anisotropic FWI, up to 12Hz including Q attenuation, was applied to this survey using the latest algorithms and methodologies. This paper presents the improved results and discusses the best strategies for determining the appropriate input data for FWI (diving-wave, reflection, or both), and depth limitation. The complete modelling required five components: diving-wave velocity updates to depths of 2200m; reflection waves included from 1600m onwards; derived anisotropic values; derived Q-model; and residual curvature tomography.

Introduction

The Vorwata field is situated in Berau Bay, Papua Barat Province in water depths of less than 70m. One objective of this case study was to improve the pressure-wave (P-wave) imaging of the Vorwata complex overburden that contains karst, shallow gas, massive carbonate intervals and complex faulting. Another objective was to improve the top and base reservoir image below 3000m, along with small fault resolution in both the reservoir and the overburden sections. It has been proven by BP (Figure 1, Schurter *et al*., 2009) from 3D finite difference modelling results in 2007 that higher resolution velocity depth modelling of the karst features gives a better image quality at the reservoir depth level.

The velocity of the karst features within the overlying thick limestone interval must be well defined to produce a good reservoir image. However, the karst shapes can be irregular and vary in size from small to large. Conventional velocity model building only captures long velocity wavelength which does not sufficiently describe the karstified area. FWI is required to improve velocity resolution.

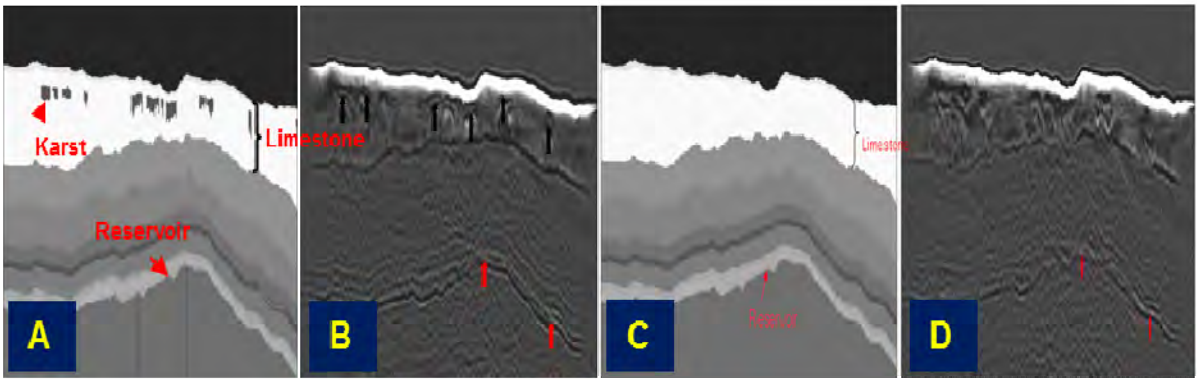

Figure 1 *A) Accurate velocity depth model. B) Pre-stack depth migration using accurate model. C) Smooth velocity depth model. D) Pre-stack depth migration using smooth model. The seismic image quality in image B at the reservoir level is better than in image D (indicated by red arrows). In addition, the karst reflections and base limestone are very sharp. (Schurter et al., 2009).*

FWI preconditioning

The test area consists of two patches of data. Hydrophone data is used without source and receiver deghosting, and without de-multiple application. Pre-processing included a Butterworth minimum-phase band-pass filter of 3-20Hz. Low frequencies are essential to avoid cycle skipping on the real and modelled gathers, requiring careful low frequency noise attenuation e.g. dipole sparse Tau-p inversion (Ray *et al*., 2014). Since surface waves are an elastic phenomenon that is not modelled by the acoustic wave equation in our FWI implementation, they must be removed before inversion.

To improve FWI accuracy, the far-field source signature was deghosted to obtain a good estimate of the source wavelet to match the observed seismic data. In this OBC survey, there are many more shots than receivers, so using the reciprocity principle, shot and receiver locations were swapped, reducing the computational cost significantly.

FWI modelling workflow

A maximum frequency of 12 Hz was chosen for the upper limit in FWI updates, this is a compromise between computational cost and the expected benefits at the higher frequencies. Depending on the local velocity, this maximum frequency should allow resolution of ~150m in the shallow section of the velocity model. The initial velocity model was from the 2009 FWI isotropic model provided by BP, with heavy smoothing (Figure 2).

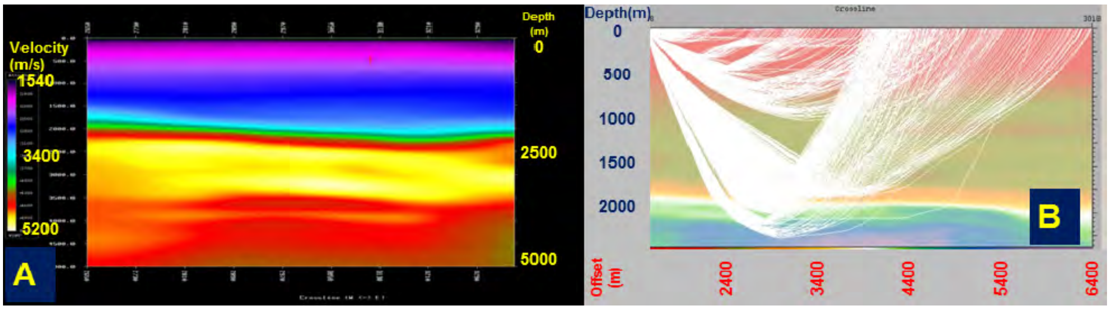

***Figure 2** A) Initial model used in FWI. B) Diving wave penetration.*

Using ray-tracing analyses, the modelling updates were divided into 4 phases. The 1st phase updates down to 2200m by using diving waves. The 2nd phase includes both diving waves and reflections to update the model from 1600m to 3600m, and integrates an anisotropic model in FWI. A joint non-linear slope tomography (Guillaume *et al*., 2008) was run to update from shallow to maximum depth in the 3rd phase. Finally, a Q-model was incorporated for the last (4th) phase.

This workflow incorporated anisotropy, a high-pass filter and limited the offsets to 3000m, allowed us to successfully performed FWI to 12Hz, which is a higher frequency than is typically described in the literature. This resulted in resolving complex features in the karst, thus improving the structure and fine details of the deeper reservoir target.

Incorporating anisotropy in FWI

Tests confirm that seismic anisotropy has to be considered in the inversion. Any anisotropic effects in the data not accounted for will otherwise be estimated as perturbations in the velocity V_0. At least one velocity and two Thomsen's parameters are needed. Although anisotropy can be inverted directly in FWI, this does require a reasonable good starting anisotropy model and there are other complicating factors involved (see, for example, da Silva *et al*., 2014; Mothi and Kumar, 2014).

Consequently, Thomsen's parameters were first derived from VSP data by 1D inversion. Since diving waves propagate nearly horizontally and are sensitive to anisotropy, they are good candidates for extracting anisotropic values. Predictability between two datasets *a* and *b* (PRED), as defined by equation 1, is known to be sensitive to changes in the earth reflectivity. Therefore, a technique was developed using diving waves that incorporates multi-layer horizon constraints to search for the best PRED between the modelled and input gathers over the entire survey to derive an initial layer-based epsilon model (Figure 3B). These anisotropic values were further refined by optimising the PRED values at each layer. For instance, to improve the match at far offsets diving waves (>3km), a decrease in epsilon is required in the layers between 1000 and 1700m, and with this, the QC Predictability maps now show values approaching 1.0 at far offsets and across all azimuths (Figure 3G).

$$PRED = \frac{\sum CC(a,b) \times CC(a,b)}{\sum AC(a) \times AC(b)} \qquad (1)$$

where CC(a,b) is the cross-correlation and AC(a,b) is the auto-correlation of datasets a and b.

Incorporating this new anisotropy model in the FWI modelling allows building of a vertical velocity model that matches reasonably with well-log velocities. It also should allow FWI to match the seismic data closer from the start, allowing for better convergence (Lin and Thomsen, 2013).

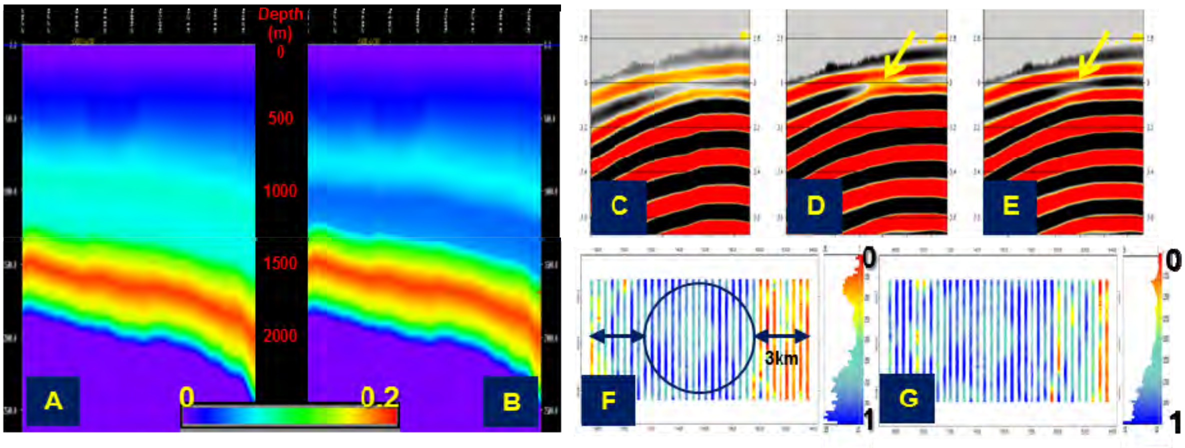

***Figure 3** A) Initial epsilon. B) Updated Epsilon. C) Raw shot. D) FWI synthetic forward shot with initial epsilon model. E) FWI synthetic forward shot with final updated Epsilon model. F) Predictability map of initial model. G) Predictability map of updated epsilon model.*

Incorporating Q-model in FWI

A Q-model derived from VSP data was provided by BP and incorporated into the ray-based migration to compensate for Q absorption. This enhanced both the CIG picking for better tomographic velocity model building, and improved FWI when reflections are included inside the inversion. The predictability map showed better matching to the raw shot when the Q-model was incorporated in the FWI inversion (Figure 4). It is also clearly seen that the fault planes and dipping events are further improved by Q-PSDM compared to application of a post-PSDM Q-compensation (Figure 5).

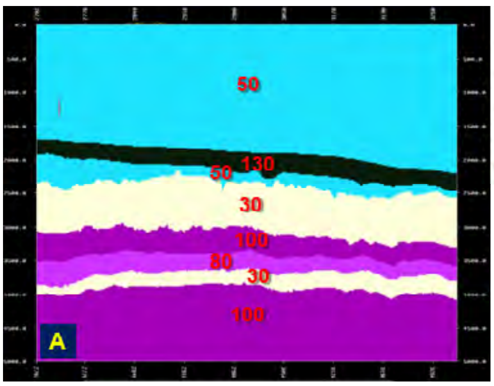

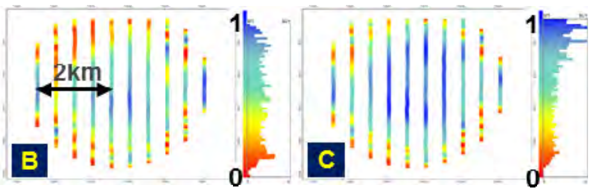

Figure 4

A) Q model provided by BP
B) Predictability without Q model
C) Predictability with Q model

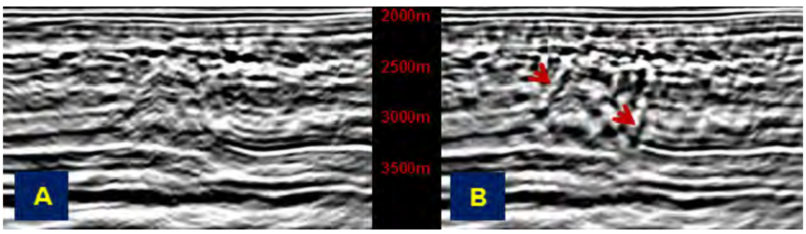

***Figure 5** A) PSDM Crossline stack with post-migration Q applied. B) Full Q-PSDM Crossline stack.*

Final result

In the final result, the new velocity model combining FWI, tomography and Q successfully imaged deep reflectors below the reservoir level at 3 to 4km depths, where events show more continuity with higher and more consistent amplitudes. Velocity details within the limestone layer appear well defined and are a reasonably good match to the well profiles. Figure 6 compares Kirchhoff PreSDM stacks using 2009 isotropic FWI and 2015 anisotropic FWI+tomo+Q models.

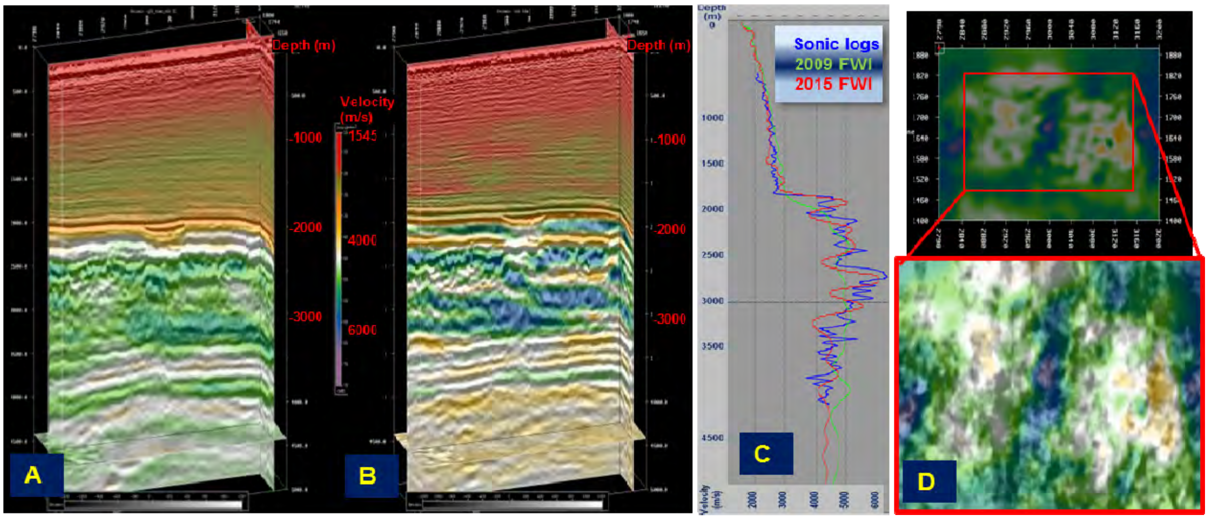

Figure 6 *A) 2009 FWI model overlaying the inline stack. B) Final FWI model overlaying the inline stack. C) Well profile. D) Final model overlaying the depth slice at 2500m, correlating with the fine details.*

Conclusions

Karst structures in the Vorwata survey create a very rugose velocity field that distorts imaging of the underlying key targets. Recent advances in FWI, along with newer velocity model building workflows, have allowed us to improve our estimate of these velocity anomalies and so improve the imaging. Including anisotropy in the FWI forward modelling and incorporating a Q model can aid FWI convergence and allow for a more accurate velocity model. Resolution was improved by increasing the FWI from 7Hz to 12Hz, but an upper limit has not yet been confirmed.

Acknowledgements

The authors would like to acknowledge SKK Migas and DitJen Migas for permission to publish this paper. We thank BP p.l.c. for providing the data and our respective companies for permission to show this work. We are also grateful to the many specialists whose shared wisdom and knowledge that are aggregated in this paper.

References

da Silva, N. V., Ratcliffe, A., Conroy, G., Vinje, V. and Body, G. [2014] A new parameterization for anisotropy update in full waveform inversion. *85th SEG Annual International Meeting*, Expanded abstract, 1050-1055.

Guillaume, P., Lambaré, G., Leblanc, O., Mitouard, P., Le Moigne, J., Montel, J.P., Prescott, A., Siliqi, R., Vidal, N., Zhang, X. and Zimine, S. [2008] Kinematic invariants: an efficient and flexible approach for velocity model building. *78th Annual SEG Meeting*, workshop "Advanced velocity model building techniques for depth imaging".

Lin, R. and Thomson, L. [2013] Extracting polar anisotropy parameters from seismic data and well logs. *SEG Houston 2013 Annual Meeting*. Expanded abstract, 310-314.

Mothi, S. and Kumar, R. [2014] Detecting and estimating anisotropy errors using full waveform inversion and ray-based tomography: A case study using long-offset acquisition in the Gulf of Mexico. *85th SEG Annual International Meeting*, Expanded abstract, 1066-1071.

Ray, S., Zhang, Z., Fu, Z., Liu, L. and Wang, P. [2014] Noise attenuation using a dipole sparse Tau-P inversion. *84th SEG Annual International Meeting*, Expanded abstract, 4213-4217.

Schurter, G.J., Supriatna, Y., Nuraeni, A., Supriyono, Regone, C.J. and Kabir, N. [2009] A 3D finite-difference modeling study of seismic imaging challenges in Bintuni Bay, Irian Jaya Barat, *The Leading Edge*, **28**, 1008-1021.